PCCP

PAPER

View Article Online
View Journal | View Issue

Cite this: *Phys. Chem. Chem. Phys.*, 2014, **16**, 5987

On the gas-phase reaction between SO_2 and $O_2^-(H_2O)_{0-3}$ clusters – an *ab initio* study†

Narcisse T. Tsona,[a] Nicolai Bork*[ab] and Hanna Vehkamäki[a]

Received 7th November 2013,
Accepted 28th January 2014

DOI: 10.1039/c3cp54715a

www.rsc.org/pccp

We present an *ab initio* investigation of the gas-phase reaction between SO_2 and a $O_2^-(H_2O)_n$ molecular cluster, n = 0–3. The associative product cluster, $O_2SO_2^-(H_2O)_n$, is formed with high energy gain although the binding energies decrease with increasing hydration. About 54 kcal mol^{-1} may be gained by isomerization of $O_2SO_2^-(H_2O)_n$ to the sulfate radical, $SO_4^-(H_2O)_n$, but a high energy barrier separates the two states. Although the isomerization is catalysed by the presence of a second SO_2 molecule, the formation of $SO_4^-(H_2O)_n$ *via* $O_2^-(H_2O)_n$ and SO_2 is found to be negligible under atmospheric conditions. At thermal equilibration at 298.15 K and 50% relative humidity the end products are mainly $O_2SO_2^-$ and $O_2SO_2^-(H_2O)_1$.

1 Introduction

Sulfuric acid (H_2SO_4) is a minor constituent in the earth's atmosphere, yet it plays a major role in several processes, *e.g.* aerosol formation and acid precipitation. The dominant source of atmospheric H_2SO_4 is oxidation of SO_2 by the well known gas-phase reactions with the hydroxyl radical, molecular O_2 and water.[1] However, evidence of alternative SO_2 oxidation mechanisms has recently been presented, driven by mineral dust, Criegee intermediates, or gaseous anions.[2–7]

The majority of free atmospheric ions originate from radon decay or from collisions between galactic cosmic rays and atmospheric N_2 or O_2. In either case, free electrons and cations are produced.[8] A free electron is extremely reactive and will, most likely, attach to O_2 due to its high concentration and positive electron affinity. The resulting species, O_2^- (superoxide ion), rapidly hydrates and may take up several water molecules depending on relative humidity and temperature.[9–11]

Using mass spectrometry, the reactivity of $O_2^-(H_2O)_n$ with several atmospheric trace gases, including SO_2, has been studied by several groups, all finding that the reaction rate of

$$SO_2 + O_2^-(H_2O)_n \rightarrow \text{Products} \qquad \text{(R1)}$$

is close to the collision rate. However, the structure of the resulting sulfur anion remains disputed. Fehsenfeld and Ferguson[12] found that the products of reaction (R1) rapidly reacted with NO_2 forming either NO_2^- or NO_3^- and suggested the molecular cluster $O_2SO_2^-$ as the primary sulfur containing product of reaction (R1). A later study by Fahey *et al.*[13] conducted in the same laboratory concluded that the product of reaction (R1) possessed "*some chemical stability exceeding that expected for purely electrostatic cluster ions*", and suggested SO_4^-. Also using mass spectrometry, Shuie *et al.*[14] specifically investigated the discrepancy concerning the outcome of reaction (R1) and found that the $O_2SO_2^-$ structure was most likely. However, due to the inherent limitations of mass spectrometry, none of these studies could provide direct insight into the reaction mechanism or into the chemical structure of the product. In later studies, the discrepancy seems to have been neglected and either SO_4^- or $O_2SO_2^-$ has been assumed without specific justification.[15–18]

Due to the elevated ion concentrations at high altitudes, reaction (R1) might be important in the high troposphere or in the stratosphere, but as shown by Fehsenfeld and Ferguson, the two proposed product structures have widely different chemical properties. Hence, firmly establishing the resulting structure is a pre-requisite for following the further chemical fate of the anion and assessing its atmospheric impact.

In the current work, reaction (R1) is studied in-depth using density functional theory (DFT) and coupled cluster calculations. We determine the most stable configurations of reactants, products and transition states (TS). We evaluate the effect of hydration on the energy barrier, and finally we analyse the distribution of the final cluster population.

2 Computational methods

The present study involves hydrated clusters of highly oxidized sulfur anions and particular care must be taken when selecting appropriate computational methods. In a series of previous

[a] *Department of Physics, University of Helsinki, P.O. Box 64, Helsinki, Finland. E-mail: nicolai.bork@helsinki.fi*
[b] *Department of Chemistry, University of Copenhagen, 2100 Copenhagen, Denmark*

† Electronic supplementary information (ESI) available. See DOI: 10.1039/c3cp54715a

studies[11,19] we have found and confirmed that the CAM-B3LYP DFT functional[20] in combination with the aug-cc-pVDZ basis set[21] yields electronic energies in good agreement with high level coupled cluster calculations. Both the CAM-B3LYP functional and the aug-cc-pVDZ basis set are particularly suitable for reproducing the diffuse nature of the extra electron in negatively charged systems and is a good compromise between accuracy and computational cost.[22]

For all of the most stable configurations of reactants, products and TS, the electronic energies were corrected by single point coupled cluster calculations. The Gibbs free energy, G, is thus calculated as

$$G = G_{\mathrm{DFT}} - E_{\mathrm{DFT}} + E^{\dagger}_{\mathrm{CC}} \quad (1)$$

where E_{DFT} and E_{CC} denote the electronic energy from DFT and coupled cluster calculations, respectively. "†" denotes that the structure is not optimized at that level of theory.

A thorough testing of coupled cluster methods and basis sets was conducted including the CCSD(T) and CCSD(T)-F12[23] methods and the cc-pVDZ (VDZ),[21] aug-cc-pVXZ (AVXZ, X = D, T, Q),[21] and VXZ-F12 (X = D, T)[24] basis sets. The testing is summarized in Table 1, showing the electronic binding energies of SO_2 and $O_2^-(H_2O)_n$ and the electronic energy barriers of the isomerization of $O_2SO_2^-(H_2O)_n$ to $SO_4^-(H_2O)_n$. It is seen that the F12 approximation significantly outperforms conventional CCSD(T) calculations with respect to basis set convergence, in particular when treating the transition states. Consequently, the CCSD(T)-F12 method with the VDZ-F12 basis set was chosen for electronic energy correction calculations. The resulting Gibbs free energies are shown in Fig. 2 and tabulated in the ESI.†

The T1 and D1 diagnostics from the CCSD(T)-F12 calculations ranged between 0.02 and 0.03, and 0.03 and 0.15, respectively, indicating low to modest multireference character of the species.

All DFT calculations and thermal corrections, using the rigid rotor and harmonic oscillator approximation, were obtained using the Gaussian 09 package.[25] All coupled cluster calculations were performed using the Molpro package.[26]

Given the small molecules and the limited amount of water (up to 3 molecules), we did not perform systematic conformational searches. In stead, initial guesses for the structures of the clusters were determined either by manually arranging all molecules or by gradually building larger clusters by adding water molecules stepwise. The structures and energies of $O_2^-(H_2O)_{0-3}$ were readily available from a previous study.[11]

The determination of TS structures followed two steps. First, we performed a series of configurational scans along the reaction coordinate with stepsize down to 0.01 Å. The structures closest to the transition state were then refined using the Synchronous Transit Quasi-Newton method (STQN).[27] The harmonic frequencies were determined for all optimized configurations, and a single imaginary frequency corresponding to the reaction coordinate was found in each TS. Further, intrinsic reaction coordinates[28] were followed from each TS to ensure its connectivity to the desired reactants and products.

Table 1 Electronic binding energies of reaction (R2) and electronic energy barriers of reaction (R3a) from the indicated method and the basis set. "n" denotes the number of water molecules included. F12 is shorthand for CCSD(T)-F12 and CAM is shorthand for CAM-B3LYP. Units are kcal mol^{-1}. See also Fig. 2

		Binding energy		Energy barrier	
Method	Basis set	n = 0	n = 1	n = 0	n = 1
CAM	AVDZ	−45.05	−36.88	40.87	36.81
CCSD(T)	VDZ	−45.76	−37.05	40.73	37.47
CCSD(T)	AVDZ	−42.03	−35.02	37.77	33.79
CCSD(T)	AVTZ	−41.36	−34.15	32.37	27.99
CCSD(T)	AVQZ	−41.50	—	30.83	—
F12	VDZ-F12	−41.17	−33.59	29.50	24.81
F12	VTZ-F12	−41.42	−33.89	29.43	24.80

3 Results and discussions

3.1 Equilibrium structures and thermodynamics

The product of a simple optimization of separated SO_2 and $O_2^-(H_2O)_n$ was found to be the $O_2SO_2^-(H_2O)_n$ molecular cluster, structurally different from the sulfate radical (SO_4^-).

Since the adiabatic electron affinity of SO_2 exceeds that of O_2 by *ca.* 15 kcal mol^{-1}, electron transfer in the unhydrated collision is readily favourable. However, due to the large difference in water affinity between O_2^- and O_2, the energy gain of electron transfer between $O_2^-(H_2O)_n$ and SO_2 is decreased by *ca.* 12.5 and 9.7 kcal mol^{-1} for n = 1 and 2, respectively.[29,30] In the de- and mono-hydrated system, it is therefore expected that the electron will transfer before the actual collision, whereas in collisions involving two or more water molecules, the electron will remain in the O_2^- moiety and transfer at some point after the collision, driven by formation of either $O_2SO_2^-$ or solvated SO_2^-.

In the presence of at least one water molecule, the reaction proceeds through a ligand switching where one H_2O in the $O_2^-(H_2O)_n$ cluster is displaced by the incoming SO_2. Due to the released energy of the clustering process, the displaced H_2O is likely to evaporate. However, due to the high concentration of atmospheric H_2O, thermal equilibrium settles very quickly and the fate of the displaced H_2O molecule is thus not imperative. For this reason, we will for simplicity consider the addition reaction.

$$SO_2 + O_2^-(H_2O)_n \rightarrow O_2SO_2^-(H_2O)_n. \quad (R2)$$

The most stable structures of $O_2SO_2^-(H_2O)_n$ are shown in Fig. 1. A new S–O bond is formed between one O_2 oxygen atom and the sulfur atom in SO_2. This S–O bond length ranges between 1.97 Å and 2.01 Å. This can be compared with the S–OH bond length of 1.63 Å in H_2SO_4 and S–O_2 bond length of 1.80 Å in SO_5^-.[6] The O–OSO_2 bond length is shortened from 1.32 Å in $O_2^-(H_2O)_n$ to 1.29 Å and is practically independent of hydration. This may be compared to 1.21 Å in molecular O_2.

The Gibbs free energy surfaces of the formation of $O_2SO_2^-(H_2O)_n$ clusters are shown in Fig. 2. These energies and further thermodynamic data are tabulated in the ESI.†

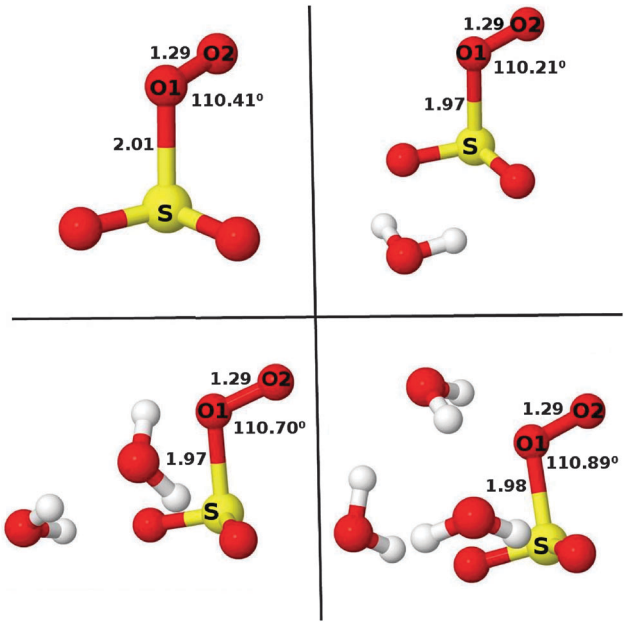

Fig. 1 Ground state structures of $O_2SO_2^-(H_2O)_{0-3}$ including some descriptive bond angles and bond lengths (in Å). Colour coding: yellow = sulphur, red = oxygen, and white = hydrogen.

The formation Gibbs free energies of $O_2SO_2^-(H_2O)_n$, henceforth denoted $\Delta G^o_{(R2)}$, are highly negative and since we found no evidence of an energy barrier, the clusters are predicted to form upon collision. Under standard conditions, the dehydrated system is formed with a Gibbs free energy gain of $\Delta G^o_{(R2)}$ = 31.2 kcal mol^{-1}. This energy gain decreases with increasing hydration due to the energy gained by O_2^- hydration, which reduces the energy gain for further clustering. $\Delta G^o_{(R2)}$ is reduced by *ca.* 10, 6, and 3.5 kcal mol^{-1} at the first, second and third hydration, respectively.

Further, the structures of $SO_4^-(H_2O)_{0-3}$ were determined and are shown in the ESI.† These structures are very similar to previously published structures of both hydrated SO_4^{2-} and hydrated SO_4^-.[31] From Fig. 2 it is seen that $SO_4^-(H_2O)_{0-3}$ is *ca.* 54 kcal mol^{-1} more stable than the corresponding $O_2SO_2^-(H_2O)_{0-3}$ clusters, regardless of the level of hydration.

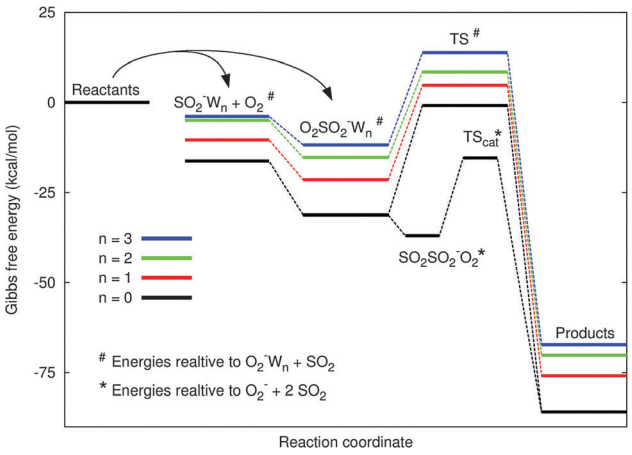

Fig. 2 Relative Gibbs free energies (298.15 K) of the species involved in reactions between SO_2 and $O_2^-(H_2O)_n$ under standard conditions. "TS" denote transition states, and "W" is shorthand for water. The SO_2 catalysed isomerisation is included for n = 0, which proceeds through TS_{cat}.

3.2 Transition states and energy barriers

We consider the following fates of the newly formed $O_2SO_2^-(H_2O)_n$ cluster,

(a) oxidation to $SO_4^-(H_2O)_n$ and

(b) decomposition into $SO_2^-(H_2O)_n$ and O_2,

according to the following reactions

$$O_2SO_2^-(H_2O)_n \rightarrow \begin{cases} SO_4^-(H_2O)_n & (a) \\ SO_2^-(H_2O)_n + O_2 & (b) \end{cases} \quad (R3)$$

Considering first the oxidation reaction, *i.e.* reaction (R3a), several TS were located between the reactant and product complexes. For each degree of hydration, the most stable one is shown in Fig. 3. We first note that the water molecules are concentrated around the breaking O1–O2 bond in the TS, whereas they are concentrated around the O_2–SO_2^- bond in the associative product clusters, shown in Fig. 1. Secondly, we find that the S–O1–O2 angle is decreased as the O2 atom is approaching the sulfur atom. Similarly, the O_2–SO_2 bond is reduced by *ca.* 0.30 Å while the O–OSO_2 bond is increased by *ca.* 0.20 Å. In general, the structure of the central ion is practically independent of the level of hydration.

The energies of these TS are included in Fig. 2. Further details, including all harmonic frequencies, are given in the ESI.† For the dehydrated system the barrier is 0.9 kcal mol^{-1} below the separate reactants and 30.4 kcal mol^{-1} above $O_2SO_2^-$. Adding a water molecule reduces the Gibbs free barrier

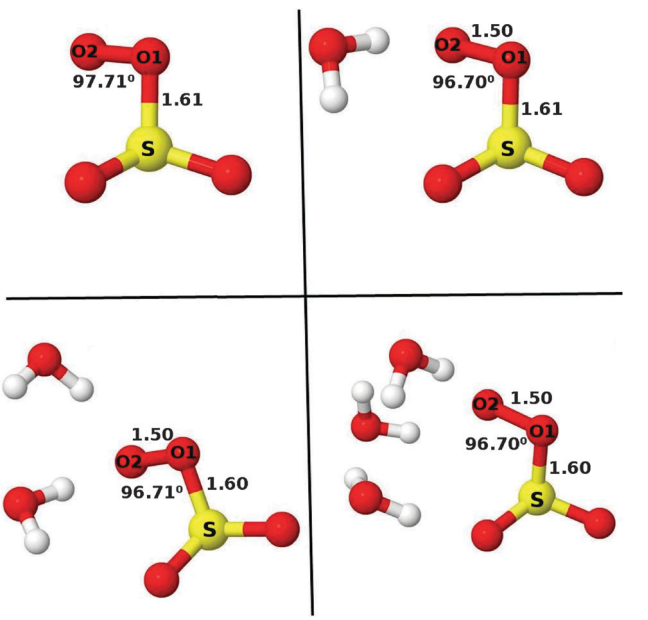

Fig. 3 Structures of the most stable TS separating the $O_2SO_2^-$ and SO_4^- states including some descriptive bond angles and bond lengths (in Å). Colour coding: yellow = sulphur, red = oxygen, and white = hydrogen.

to 26.2 kcal mol^{-1} while adding another water molecule reduces the barrier further to 23.8 kcal mol^{-1}. A third water molecule slightly increases the barrier to 25.6 kcal mol^{-1} above the reactant complex.

Next, reaction (R3b) was studied (the optimized $SO_2^-(H_2O)_n$ structures are shown in the ESI†). Similar to the formation of $O_2SO_2^-$ from O_2^- and SO_2, no evidence of a transition state for the breakup of $O_2SO_2^-$ into SO_2^- and O_2 was found. The dehydrated reaction is the least favourable with $\Delta G^{o}_{(R3b)}$ = 14.9 kcal mol^{-1}. Adding one, two, and three water molecules is seen to increasingly shift the equilibrium towards the products although the Gibbs free reaction energies remain decisively positive. Also these energies are included in Fig. 2, and further details are given as ESI.†

Comparing the energy barriers of reactions (R3a) and (R3b), it is immediately clear that the high energy barriers of reaction (R3a) effectively hinder any SO_4^- formation. More likely, the $O_2SO_2^-(H_2O)_n$ molecular complexes will instead dissociate by O_2 and/or H_2O evaporation resulting from the large release of potential energy from reaction (R2). A kinetic model including reactions (R2), (R3a), and (R3b), and assuming the steady state of $O_2SO_2^-(H_2O)_n$,[19] showed that the fraction of collisions leading to SO_4^- formation, in all cases, was below 10^{-7}. Details are presented as ESI.†

3.3 Effect of a second SO_2 molecule

Although we reject the atmospheric significance of SO_4^- formation initiated by O_2^- clusters, the conclusion of Fahey *et al.*[13] remains interesting since it suggests that secondary reactions may have taken place in the experimental setup. This idea is further supported by the similarities between the $O_2SO_2^-$ core ion and the group of Criegee intermediates (CI), R_2COO. Like $O_2SO_2^-$, CI's contain a terminal peroxide group and the CI electronic structure may be described as both zwitterionic and biradical. Upon collision with Criegee biradicals, SO_2 may either oxidize to SO_3 or catalyze the isomerization of the Criegee biradical to a carboxylic acid.

Hereby motivated, we investigated the reaction

$$O_2SO_2^- + SO_2 \rightarrow SO_3^- + SO_3 \qquad (R4)$$

but at the CAM-B3LYP/aug-cc-pVDZ level of theory, a Gibbs free energy barrier of more than 120 kcal mol^{-1} is found between the reactants and products. Reaction (R4) is thus insignificant under any conditions.

We also investigate the possibility of SO_2 catalysing the isomerization of $O_2SO_2^-$ to SO_4^- *via*

$$O_2SO_2^- + SO_2 \rightarrow O_2SO_2SO_2^- \rightarrow SO_4^- + SO_2 \qquad (R5)$$

The clustering reaction of $O_2SO_2^- + SO_2$ was found to be exothermic by 5.74 kcal mol^{-1}, in good agreement with 6.23 kcal mol^{-1} found experimentally by Vacher *et al.*[32] This indicate that under pristine atmospheric conditions, *e.g.* p(SO_2) = 2 ppb, less than 0.01% of the $SO_2O_2^-$ clusters bind an additional SO_2 molecule. Considering the dehydrated isomerization reaction only, we identified a transition state 21.0 kcal mol^{-1} above the $O_2SO_2SO_2^-$ complex and 15.5 kcal mol^{-1} above the separated reactants, as shown in Fig. 2. The transition state involves the simultaneous transferring of two oxygen atoms, and is shown in Fig. 4. Although the transition state is structurally similar to the corresponding Criegee based transition state, also shown in Fig. 4, the barrier is much larger and effectively hinders this reaction as well.

3.4 Equilibrium with O_2 and H_2O

As hereby demonstrated, the $O_2SO_2^-$ molecular cluster is chemically stable towards oxidation to SO_4^- and its chemical fate will depend on other reactants, *e.g.* other oxidants, acids, or radicals. Due to the low concentrations of such species, these reactions will occur after thermal equilibrium has settled. This will be considered *via* the following reactions

$$O_2SO_2^-(H_2O)_n + H_2O \leftrightarrow O_2SO_2^-(H_2O)_{n+1} \qquad (R6)$$

$$SO_2^-(H_2O)_n + H_2O \leftrightarrow SO_2^-(H_2O)_{n+1} \qquad (R7)$$

$$SO_2^-(H_2O)_n + O_2 \leftrightarrow O_2SO_2^-(H_2O)_n. \qquad (R8)$$

Their thermodynamics are shown in Fig. 5 and tabulated in the ESI.†

Considering first the equilibria with water, we find that hydration of both SO_2^- and $O_2SO_2^-$ is thermally favourable under atmospheric conditions although the energy gain decreases with increasing hydration. The first hydration is the most favorable, with ΔG° = −6.8 kcal mol^{-1} and −2.9 kcal mol^{-1} for SO_2^- and $O_2SO_2^-$, respectively. The second and third hydration energies for both SO_2^- and $O_2SO_2^-$ are above the critical clustering energy given by $RT \times \ln([H_2O])$ = −2.5 kcal mol^{-1} (T = 298.15 K and 50% relative humidity). This signifies that the monohydrated clusters are the most abundant.[11]

For the dehydrated system, reaction (R8) is exothermic with $\Delta G^{o}_{(R8)}$ = 14.9 kcal mol^{-1} in good agreement with −15.5 kcal mol^{-1} found experimentally by Shuie *et al.*[14] At increasing hydration, this value becomes less negative, but remains much below the critical clustering energy at $RT \times \ln([O_2])$ = −1.0 kcal mol^{-1} (T = 298.15 K and $[O_2]$ = 0.2 bar), implying that the $O_2SO_2^-$ ion is stable under atmospheric conditions.

Assuming that thermal equilibrium has been reached we use the law of mass action,

$$\frac{[O_2SO_2^-(H_2O)_{n+1}]}{[O_2SO_2^-(H_2O)_n]} = [H_2O] \times \exp\left(-\frac{\Delta G}{RT}\right), \qquad (2)$$

where the chemical activities are approximated by vapor pressures. Eqn (2) is for reaction (R6), and analogous equations are

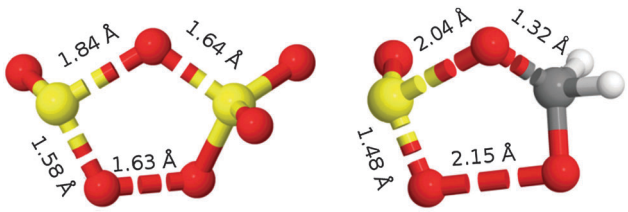

Fig. 4 Left: transition state structure of the SO_2 catalyzed $O_2SO_2^-$ to SO_4^- isomerization. Right: transition state structure of the SO_2 catalyzed Criegee intermediate (CH_2O_2) to formic acid isomerization.[33]

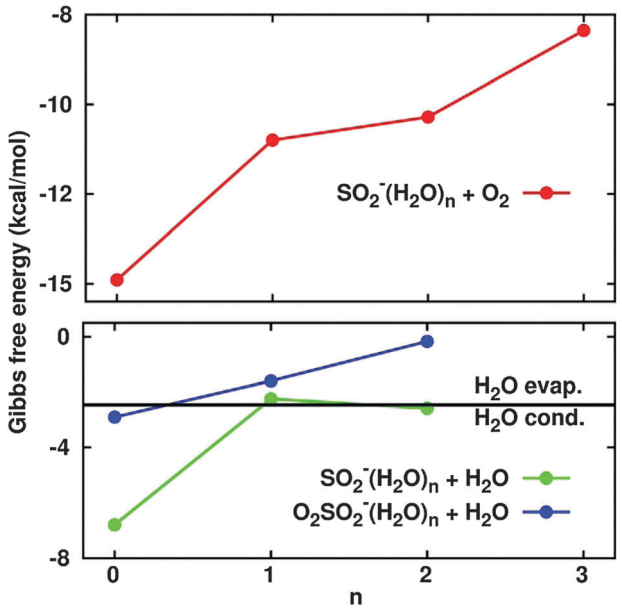

Fig. 5 Gibbs free energies for reactions (R6)–(R8) representing the growth of clusters *via* H_2O condensation (lower panel) and O_2 condensation (upper panel). The domains of H_2O evaporation and condensation are determined under standard conditions and 50% relative humidity.

valid for reactions (R7) and (R8). At T = 298.15 K and 50% relative humidity we thus find that the system equilibrium consists of 58% $O_2SO_2^-(H_2O)_1$, 28% $O_2SO_2^-$, and 13% $O_2SO_2^-(H_2O)_2$, while the remainder constitutes about 1% of the cluster population.

4 Conclusions

Using *ab initio* calculations, we have investigated the reaction between SO_2 and $O_2^-(H_2O)_n$ and established its most likely products. In accordance with several experiments, we find that the electron is immediately transferred from O_2^- to SO_2 with high energy gain whereafter a $O_2SO_2^-$ cluster is formed.

Regardless of hydration, isomerization of $O_2SO_2^-$ to SO_4^- is effectively hindered by a high energy barrier. Although a second SO_2 molecule may catalyse the $O_2SO_2^-$ isomerization, this process is extremely slow. This despite the transition state is structurally similar to the transition state in the corresponding reaction between SO_2 and the Criegee intermediate, H_2COO, which is known to be *ca.* 13 kcal mol^{-1} below the separated reactants.[33]

We are thus unable to identify any reaction mechanisms connecting SO_2^- to SO_4^- fast enough to contribute measurably under conditions relevant in the atmosphere or in a typical experimental setup. Although we cannot categorically dismiss the reports of SO_4^- from SO_2^- based clusters, either directly or through some secondary reactions, our findings strongly suggest that the major outcome of a collision between O_2^- and SO_2 is $O_2SO_2^-$. Under atmospheric conditions (T = 298.15 K, RH = 50%) the main products are $O_2SO_2^-(H_2O)_1$, $O_2SO_2^-$, and $O_2SO_2^-(H_2O)_2$, constituting, 58, 28, and 13% of the population, respectively.

Acknowledgements

We thank Dr Theo Kurtén for valuable scientific discussions and acknowledge the Academy of Finland (LASTU program project number 135054), ERC project 257360-MOCAPAF, and the Villum foundation for funding. We acknowledge the CSC-IT Centre for Science in Espoo, Finland for computer time.

References

1 J. H. Seinfeld and S. N. Pandis, *Atmospheric Chemistry and Physics: From Air Pollution to Climate Change*, Wiley, New Jersey, 2nd edn, 2006.
2 E. Harris, B. Sinha, D. van Pinxteren, A. Tilgner, K. W. Fomba, J. Schneider, A. Roth, T. Gnauk, B. Fahlbusch, S. Mertes, T. Lee, J. Collett, S. Foley, S. Borrmann, P. Hoppe and H. Herrmann, *Science*, 2013, **340**, 727–730.
3 L. Vereecken, H. Harder and A. Novelli, *Phys. Chem. Chem. Phys.*, 2012, **14**, 14682–14695.
4 O. Welz, J. D. Savee, D. L. Osborn, S. S. Vasu, C. J. Percival, D. E. Shallcross and C. A. Taatjes, *Science*, 2012, **335**, 204–207.
5 M. B. Enghoff and H. Svensmark, *Atmos. Chem. Phys.*, 2008, **8**, 4911–4923.
6 N. Bork, T. Kurtén and H. Vehkamäki, *Atmos. Chem. Phys.*, 2013, **13**, 3695–3703.
7 N. Bork, V. Loukonen and H. Vehkamäki, *J. Phys. Chem. A*, 2013, **117**, 3143–3148.
8 G. Bazilevskaya, I. Usoskin, E. Flückiger, R. Harrison, L. Desorgher, R. Bütikofer, M. Krainev, V. Makhmutov, Y. Stozhkov, A. Svirzhevskaya, N. Svirzhevsky and G. Kovaltsov, *Space Sci. Rev.*, 2008, **137**, 149–173.
9 T. Seta, M. Yamamoto, M. Nishioka and M. Sadakata, *J. Phys. Chem. A*, 2003, **107**, 962–967.
10 N. Y. Antonchenko and E. S. Kryachko, *Ukr. J. Phys.*, 2006, **51**, 27–38.
11 N. Bork, T. Kurtén, M. B. Enghoff, J. O. P. Pedersen, K. V. Mikkelsen and H. Svensmark, *Atmos. Chem. Phys.*, 2011, **11**, 7133–7142.
12 F. Fehsenfeld and E. Ferguson, *J. Chem. Phys.*, 1974, **61**, 3182–3193.
13 D. W. Fahey, H. Böhringer, F. Fehsenfeld and E. Ferguson, *J. Chem. Phys.*, 1982, **76**, 1799–1805.
14 L.-R. Shuie, E. D. D'sa, W. E. Wentworth and E. C. Chen, *Struct. Chem.*, 1993, **4**, 213–218.
15 O. Möhler, T. Reiner and F. Arnold, *J. Chem. Phys.*, 1992, **97**, 8233–8239.
16 J. R. Vacher, M. Jorda, E. L. Duc and M. Fitaire, *Int. J. Mass Spectrom. Ion Processes*, 1992, **114**, 149–162.
17 V. K. Lakdawala and J. Moruzzi, *J. Phys. D: Appl. Phys.*, 1981, **14**, 2015.
18 X. Yang and A. Castleman Jr, *J. Phys. Chem.*, 1991, **95**, 6182–6186.
19 N. Bork, T. Kurtén, M. Enghoff, J. Pedersen, K. Mikkelsen and H. Svensmark, *Atmos. Chem. Phys.*, 2012, **12**, 3639–3652.
20 T. Yanai, D. P. Tew and N. C. Handy, *Chem. Phys. Lett.*, 2004, **393**, 51–57.

21 T. H. Dunning, *J. Chem. Phys.*, 1989, **90**, 1007–1023.
22 T. Seta, M. Yamamoto, M. Nishioka and M. Sadakata, *J. Phys. Chem. A*, 2003, **107**, 962–967.
23 T. B. Adler, G. Knizia and H. J. Werner, *J. Chem. Phys.*, 2007, **127**, 221106.
24 K. A. Peterson, T. B. Adler and H.-J. Werner, *J. Chem. Phys.*, 2008, **128**, 084102.
25 M. J. Frisch, G. W. Trucks, H. B. Schlegel, G. E. Scuseria, M. A. Robb, J. R. Cheeseman, G. Scalmani, V. Barone, B. Mennucci, G. A. Petersson, H. Nakatsuji, M. Caricato, X. Li, H. P. Hratchian, A. F. Izmaylov, J. Bloino, G. Zheng, J. L. Sonnenberg, M. Hada, M. Ehara, K. Toyota, R. Fukuda, J. Hasegawa, M. Ishida, T. Nakajima, Y. Honda, O. Kitao, H. Nakai, T. Vreven, J. A. Montgomery Jr., J. E. Peralta, F. Ogliaro, M. Bearpark, J. J. Heyd, E. Brothers, K. N. Kudin, V. N. Staroverov, T. Keith, R. Kobayashi, J. Normand, K. Raghavachari, A. Rendell, J. C. Burant, S. S. Iyengar, J. Tomasi, M. Cossi, N. Rega, J. M. Millam, M. Klene, J. E. Knox, J. B. Cross, V. Bakken, C. Adamo, J. Jaramillo, R. Gomperts, R. E. Stratmann, O. Yazyev, A. J. Austin, R. Cammi, C. Pomelli, J. W. Ochterski, R. L. Martin, K. Morokuma, V. G. Zakrzewski, G. A. Voth, P. Salvador, J. J. Dannenberg, S. Dapprich, A. D. Daniels, O. Farkas, J. B. Foresman, J. V. Ortiz, J. Cioslowski and D. J. Fox, *Gaussian 09, Revision C.01*, Gaussian, Inc., Wallingford, CT, 2010.
26 H.-J. Werner, P. J. Knowles, G. Knizia, F. R. Manby, M. Schtz, P. Celani, T. Korona, R. Lindh, A. Mitrushenkov, G. Rauhut, K. R. Shamasundar, T. B. Adler, R. D. Amos, A. Bernhardsson, A. Berning, D. L. Cooper, M. J. O. Deegan, A. J. Dobbyn, F. Eckert, E. Goll, C. Hampel, A. Hesselmann, G. Hetzer, T. Hrenar, G. Jansen, C. Kppl, Y. Liu, A. W. Lloyd, R. A. Mata, A. J. May, S. J. McNicholas, W. Meyer, M. E. Mura, A. Nicklass, D. P. O'Neill, P. Palmieri, D. Peng, K. Pflger, R. Pitzer, M. Reiher, T. Shiozaki, H. Stoll, A. J. Stone, R. Tarroni, T. Thorsteinsson and M. Wang, *MOLPRO, version 2012.1, a package of ab initio programs*, 2012, see http://www.molpro.net.
27 C. Peng, P. Ayala, H. Schlegel and M. Frisch, *J. Comput. Chem.*, 1996, **17**, 49–56.
28 K. Fukui, *Acc. Chem. Res.*, 1981, **14**, 363–368.
29 M. Arshadi and P. Kebarle, *J. Phys. Chem.*, 1970, **74**, 1483–1485.
30 A. J. Bell and T. G. Wright, *Phys. Chem. Chem. Phys.*, 2004, **6**, 4385–4390.
31 M. L. McKee, *J. Phys. Chem.*, 1996, **100**, 3473–3481.
32 J. Vacher, E. Le Duc and M. Fitaire, *Int. J. Mass Spectrom. Ion Processes*, 1994, **135**, 139–153.
33 T. Kurtén, J. R. Lane, S. Jørgensen and H. G. Kjaergaard, *J. Phys. Chem. A*, 2011, **115**, 8669–8681.

